

POTENTIAL CHEMOTHERAPEUTIC ACTIVITY OF  
4-iodo-3-nitrobenzamideMETABOLIC REDUCTION TO THE 3-NITROSO DERIVATIVE AND  
INDUCTION OF CELL DEATH IN TUMOR CELLS IN CULTUREJEROME MENDELEYEV, EVA KIRSTEN, ALAEDDIN HAKAM,  
KALMAN G. BUKI and ERNEST KUN\*Laboratory for Environmental Toxicology and Chemistry and the Octamer Research Foundation,  
Romberg Tiburon Centers, San Francisco State University, Tiburon, CA 94920, U.S.A.

(Received 7 December 1994; accepted 2 March 1995)

**Abstract**—A C-nitroso prodrug, 4-iodo-3-nitrobenzamide, was synthesized, and its action on a variety of tumor cells of human and animal origin tested. This prodrug was reduced transiently by tumor cells to 4-iodo-3-nitrosobenzamide at a very low rate, which was, however, sufficient to kill tumor cells. The final reduction product was 4-iodo-3-aminobenzamide, and no intermediates accumulated. No toxicity could be observed in hamsters even at 200 mg/kg, given i.p. daily for 7 days. The chemical reactivity of both 4-iodo-3-nitrosobenzamide and its noniodinated homolog with reduced ascorbate yielded the hydroxylamines. With glutathione, 4-iodo-3-aminobenzamide was formed, suggesting glutathione sulfinic acid formation. Confirming earlier studies, 4-iodo-3-nitrosobenzamide inactivated poly(ADP-ribose) polymerase by zinc ejection from the first zinc finger of this nuclear protein. The iodinated nitroso compound was more effective than its iodine-free analog. Selective tumoricidal action appeared to correlate with the reduction of the nitro group to nitroso in tumor cells, and with the previously described subsequent induction of tumor apoptosis by the C-nitroso intermediate. These processes were accelerated by buthionine sulfoximine, which diminishes cellular GSH.

**Key words:** poly(ADP-ribose) polymerase; 4-iodo-3-nitrobenzamide; metabolism; tumor cells; zinc finger

The retroviral type (CCHC) zinc fingers of the eukaryotic nuclear enzyme pADPRT<sup>†</sup> (EC 2.4.2.30) and of the p7 of nucleocapsid of HIV and SIV viruses have been shown to be selectively oxidized by aromatic C-nitroso molecules with consequent zinc ejection, resulting in loss of pADPRT activity and of retroviral infectivity [1–5]. Inactivation of pADPRT by this mechanism also induces apoptosis in tumor cells [6]. These results provide a new chemotherapeutic approach to both cancer and retroviral diseases. However, the relative chemical instability of aromatic C-nitroso group-containing pADPRT ligands, specifically toward ascorbate and GSH, is a distinct disadvantage for their direct application *in vivo*. We subsequently prepared a cysteine sulfinic acid adduct of 3-nitrosobenzamide

[7], which at weakly basic conditions releases the C-nitroso molecule; this adduct is an effective C-nitroso donor molecule in cell cultures, but its *in vivo* efficacy has not been determined. An alternate method is to prepare prodrugs that can be converted in the cell to the active C-NO molecule. A prototype of these drugs is INO<sub>2</sub>BA, a relatively stable molecule with a shelf-life at room temperature of at least 1 year, which is reduced enzymatically within tumor cells to INOBA at a slow but steady rate sufficient to kill tumor cells or to inactivate SIV or HIV viruses. In the present paper, we analyze the metabolism and tumor cell death-inducing mechanism of INO<sub>2</sub>BA in cell cultures. In a preliminary note, we reported a comparison of the anti-SIV activity and cytotoxicity of NOBA and INO<sub>2</sub>BA on CEM-174 cells [8].

\* Corresponding author: Dr. Ernest Kun, Laboratory for Environmental Toxicology and Chemistry and the Octamer Research Foundation, Romberg Tiburon Centers, San Francisco State University, 3150 Paradise Drive, P.O. Box 855, Tiburon, CA 94920. Tel. (415) 435-8851; FAX (415) 435-8853.

<sup>†</sup> Abbreviations: pADPRT, poly(ADP-ribose) polymerase; INO<sub>2</sub>BA, 4-iodo-3-nitrobenzamide; INOBA, 4-iodo-3-nitrosobenzamide; INHOHBA, 4-iodo-3-hydroxylaminobenzamide; INH<sub>2</sub>BA, 4-iodo-3-aminobenzamide; NOBA, 3-nitrosobenzamide; GSH, reduced glutathione; BSO, DL-buthionine-[S,R]-sulfoximine; EI, electron impact; DMF, *N,N*-dimethylformamide; and THF, tetrahydrofuran.

## MATERIALS AND METHODS

## Chemicals

4-Iodo-3-nitrobenzoic acid was purchased from Chemica Alta, Ltd. (Edmonton, Alberta). Thionyl chloride, peracetic acid and 3-aminobenzamide were obtained from the Aldrich Chemical Co. (Milwaukee, WI), and zinc metal dust was obtained from the Spectrum Chemical Mfg. Corp. (Gardena, CA). L-Ascorbic acid, GSH and BSO were purchased from the Sigma Chemical Co. (St. Louis, MO). All other chemicals were of the highest analytical purity.

### Instrumentation

$^1\text{H}$  NMR spectra were measured on a 360 MHz instrument by Acorn NMR (Fremont, CA), EI and FAB mass spectra at the Mass Spectrometry Laboratory, University of California (Berkeley, CA), microanalysis by Schwarzkopf Microanalytical Laboratory (Woodside, NY), UV-Vis absorption spectra (in EtOH) on a Perkin-Elmer model 552 instrument, HPLC using Waters (Milford, MA) model 6001 solvent delivery pumps and model 680 gradient controller, and a Hewlett-Packard (Santa Clara, CA) model 1040A diode-array detector with ChemStation.

### Chemical synthesis

**Synthesis of  $\text{INO}_2\text{BA}$ .** As previously described,\* 4-iodo-3-nitrobenzoic acid in DMF was amidated by treatment sequentially with excess thionyl chloride and concentrated ammonium hydroxide. The amide precipitated from aqueous solution and was crystallized from EtOH. Yields were typically 40%, m.p. 154–156°. High-resolution EIMS: calcd. for  $\text{C}_7\text{H}_5\text{N}_2\text{O}_3\text{I}$ : 291.9345; found:  $\text{M}^+$  ( $m/z$ ): 291.9349 (deviation =  $-1.4$  ppm).  $^1\text{H}$  NMR (DMSO- $d_6$ )  $\delta$  (ppm): 7.69 (1H, s), 7.86 (1H, dd,  $J = 8.2$  Hz,  $J = 1.8$  Hz), 8.23 (2H, s overlapping d,  $J = 8.1$  Hz) and 8.36 (1H, d,  $J = 1.8$  Hz). UV: max 308, 242, and 208 nm.

**Synthesis of  $\text{INH}_2\text{BA}$ .**  $\text{INO}_2\text{BA}$  (730 mg, 2.50 mmol) was dissolved in warm EtOH (25 mL) to which was then added  $\text{H}_2\text{O}$  (25 mL) at 24° followed by 1 M sodium dithionite (50 mL, freshly prepared in 0.05 M sodium bicarbonate). After 15 min, the product was extracted into ethyl acetate, which was then removed by rotary evaporation, and the residue crystallized from hot  $\text{H}_2\text{O}$  (40 mL). Yield: 139 mg (21%), m.p. 175–180° (decomp). This amino compound does not form a hydrochloride. Microanalysis: calcd. for  $\text{C}_7\text{H}_7\text{N}_2\text{O}$ : C, 32.08; H, 2.69; I, 48.43; N, 10.69. Found: C, 31.57; H, 2.37; I, 48.70; N, 10.02.  $^1\text{H}$  NMR (DMSO- $d_6$ )  $\delta$  (ppm): 5.30 (2H, multiplet, amino protons), 6.79 (1H, dd,  $J = 8.2$  Hz,  $J = 1.9$  Hz), 7.17 (1H, s), 7.23 (1H, d,  $J = 1.9$  Hz), 7.60 (1H, d,  $J = 8.0$  Hz), 7.75 (1H, s). UV: max 322 and 230 nm and shoulders at 252 and 220 nm.

**Synthesis of  $\text{INOBA}$ .** The method differs from that for 3-nitrosobenzamide [10], requiring a different oxidant. In a procedure favoring oxidation to the nitroso state, each of 20 test tubes (13  $\times$  100 mm) was charged with 5.2 mg (0.020 mmol) of  $\text{INH}_2\text{BA}$  and 0.100 mL of absolute EtOH. Each tube was heated briefly to dissolve the amino compound, followed immediately by  $\text{H}_2\text{O}$  (0.400 mL) and then peracetic acid reagent (0.400 mL, 32% in dilute

acetic acid) added at a fast drip during 10 sec. After 2 min, ethyl acetate (2.0 mL) and  $\text{H}_2\text{O}$  (2.0 mL) were added, and the mixture was vortexed and then stored on ice while the other tubes were identically processed. The upper (ethyl acetate) layers were pooled, the solution was concentrated (rotary evaporation) to 4 mL,  $\text{H}_2\text{O}$  was added until turbid, and the reaction mixture was incubated in 2° for 10 Hr. The product deposited as a light tan solid. Yield: 35.3 mg (32%), m.p. 174–176° (decomp). High resolution EIMS: calcd for  $\text{C}_7\text{H}_5\text{N}_2\text{O}_3\text{I}$ : 275.9396; found  $\text{M}^+$  ( $m/z$ ): 275.9399 (deviation =  $-0.3$  ppm).  $^1\text{H}$  NMR (DMSO- $d_6$ )  $\delta$  (ppm): 6.65 (1H, d,  $J = 2.2$  Hz), 7.60 (1H, s), 8.02 (1H, dd,  $J = 8.1$  Hz,  $J = 2.2$  Hz), 8.18 (1H, s), 8.50 (1H, d,  $J = 2.2$  Hz). UV: max 370, 252 and 226 nm and shoulders at 315 and 293 nm. Vis: max 750 nm.

**Synthesis of  $\text{INHOHBA}$ .** To a rapidly stirred solution of  $\text{INO}_2\text{BA}$  (292 mg, 1.0 mmol) in THF (25 mL) to which an aqueous solution (25 mL) of  $\text{CaCl}_2$  (220 mg, 2.0 mmol) had been added, zinc metal dust (total of 6000 mg) was added in small portions (about 50 mg each) every 30–45 sec during a period of 75 min at 24°. The mixture was filtered through celite, concentrated to 20 mL by rotary evaporation, and the product extracted into ethyl acetate (3  $\times$  50 mL). After removal of solvent, the crude residue was taken up in a mixture of EtOH (2 mL) and ethyl acetate (13 mL), and a 12-mL portion was purified on a group of six preparative TLC plates. With  $R_f = 0.61$ , the product bands were removed from the plates, extracted into ethyl acetate, and pooled. Upon concentrating to 6 mL and cooling ( $-15^\circ$ ), the product deposited as a white solid. Yield: 32.7 mg (12%), m.p. 130–133° (decomp). Low resolution FABMS displayed both  $\text{M}^+$  and  $\text{MH}^+$  peaks. High resolution FABMS: calcd. for  $\text{C}_7\text{H}_7\text{N}_2\text{O}_3\text{I}$ : 277.955230; found  $\text{M}^+$  ( $m/z$ ): 277.955070 (deviation = 0.6 ppm).

**Synthesis of 6,6'-diiodo-3,3'-dicarbamoylazoxybenzene.** To a solution of  $\text{INH}_2\text{BA}$  (209.6 mg, 0.80 mmol) in DMF (4.0 mL) at 24° was added chilled (3°) peracetic acid reagent (0.260 mL, 2 equiv). The DMF solution was combined with ethyl acetate (50 mL) and extracted with  $\text{H}_2\text{O}$  (2  $\times$  25 mL); the ethyl acetate solution was concentrated to 20 mL, DMF (1.0 mL) was added to dissolve turbidity, and the solution was subjected to preparative TLC on a set of ten plates. Using ethyl acetate, the low-mobility component ( $R_f = 0.34$ ) was isolated from the plates and pooled, and evaporation gave 20.4 mg of solid yellow residue. After redissolving in 50 mL of ethyl acetate: EtOH (10:1 v/v), concentrating to 20 mL (rotary evaporation) and cooling (2°), a small crop of crystalline product was deposited (18 hr). Yield: 4.6 mg (2%), m.p. 285–288° (decomp). High-resolution FABMS: calcd for  $\text{C}_{14}\text{H}_{11}\text{N}_4\text{O}_3\text{I}_2$ : 536.892069; found  $\text{MH}^+$  ( $m/z$ ): 536.892620 (deviation =  $-1.0$  ppm). UV: max 251 nm and shoulder at 303 nm. Analytical TLC showed that a mother liquor component from the above crystallization mixture migrated slightly faster (0.02  $R_f$  units) than the crystallized product, possibly due to the presence of a structural isomer.

**NOBA.** This compound was prepared according to a previous procedure.†

\* Kun E, Mendeleyev J and Kirsten E, Novel aromatic nitro and nitroso compounds and their metabolites, useful as antiviral and antitumor agents. *US Patent Ser. No. 08/070,313*, 1993, pending.

† Kun E, Mendeleyev J and Rice WG, Adenosine diphosphoribose polymerase binding nitroso aromatic compounds useful as retroviral inactivating agents, anti-retroviral agents and anti-tumor agents. *US Patent Ser. No. 08/087,566*, 1993, pending.

### TLC

Analytical TLC was performed on Whatman PE SIL G/UV flexible plates, using *n*-hexane:ethyl acetate:EtOH (3:1:0.8, by vol.) as mobile phase, and preparative TLC on Whatman silica gel (1000  $\mu$ m layer) 20  $\times$  20 cm plates with fluorescent indicator, using the same mobile phase. In all cases, bands were visualized under UV light.

### Chemical reactivity of NOBA and INOBA with reduced ascorbic acid and with GSH

Each nitroso compound (0.15 mmol) was dissolved in DMF (0.200 mL) to which was then added EtOH (0.800 mL) and distilled H<sub>2</sub>O (1.000 mL) to provide a stock solution (7.5 mM); aliquots (0.100 mL) were subjected to addition (0.030 mL) of solution containing either 10 equiv or 1 equiv of reagent (ascorbic acid or GSH, in distilled H<sub>2</sub>O or in 100 mM potassium phosphate adjusted to pH 7.4), at 25° with complete vortexing. The solutions were monitored by spotting on analytical TLC after 10 min, 1 hr, 4 hr and 22 hr. Products were identified by co-chromatography with known standards, and relative amounts of products were estimated by intensity of spots under UV light. The GSH adducts of the nitroso compounds were immobile on the TLC plates, clearly observed at the origin line under UV light. After 22 hr, the final products in the reaction solutions were extracted into ethyl acetate and re-spotted against standards to confirm identification.

### pADPRT inactivation and zinc-ejection by NOBA and by INOBA

These assays were performed according to the methods reported previously [1] except that the pH was 7.0. Criteria of homogeneity were as reported [9].

### Cell culture

(A) For cell lines growing in suspension culture, cells were seeded at densities of 0.1 to 0.2  $\times 10^6$ /mL into wells of 24-well plates using the appropriate recommended growth media. Drugs were added to the wells immediately after seeding, from 10–40 mM stock solutions in DMSO; BSO, when tested, was added from a 100 mM aqueous stock solution. Cells were incubated at 37° in a 5% CO<sub>2</sub> atmosphere, and cell growth and survival were evaluated in 24-hr intervals by hemacytometer counting in aliquots taken from the wells and supplemented with trypan blue. For evaluation of drug effects on DNA-unwinding, cells were seeded at a density of 0.2  $\times 10^6$ /mL (4  $\times 10^6$ /flask), drugs were added at

the time of seeding, and after 20 hr of incubation the fluorescence assay for DNA-unwinding was by a published method [10] as adopted in a previous report [6].

(B) For cell lines maintainable in monolayer culture, experiments were started by cell seeding into 2-cm<sup>2</sup> wells at densities of 0.01 to 0.02  $\times 10^6$ /cm<sup>2</sup>, drugs were added after 4–5 hr of incubation (37°, 5% CO<sub>2</sub>) to allow cell attachment, and incubation was continued for the time periods indicated (see figure legends). For assessment of drug effects, cells were detached using 0.3 mL well of 0.05% trypsin, 0.02% EDTA in balanced salt solution, supplemented with trypan blue, gently pipetted to yield single-cell suspensions, and counted in a hemacytometer.

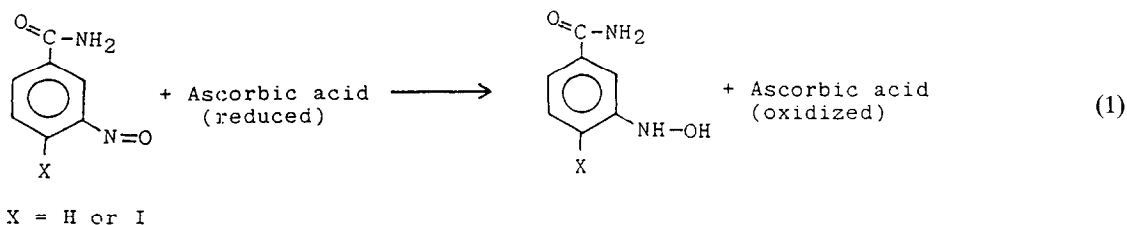
### Cell metabolism of INO<sub>2</sub>BA

A suspension of 855-2 cells [6], 150  $\times 10^6$  cells in 30 mL of RPMI-1640 medium, was dosed with INO<sub>2</sub>BA to a concentration of 120  $\mu$ M, incubated at 37° for 18 hr, and then freeze-dried, extracted three times with EtOH (10 mL each time) for 30 min, and centrifuged. The extract was rotary evaporated to dryness, redissolved in EtOH (3.0 mL), and microfuged to remove small particles; then aliquots (200  $\mu$ L) were injected into HPLC. In control experiments, instead of incubating the drug-dosed cell suspension, it was immediately frozen, freeze-dried, and extracted. HPLC analyses were performed essentially as reported earlier [1] except that the pH of the buffers was 4.3. Upon sample injection, the gradient started from 100% A to 100% B in 30 min, to 50% B/50% C in 15 min, to 100% C in 3 min (A = 0.05 M potassium phosphate, pH 4.3; B = same as A + 30% methanol; C = 50% acetonitrile and 50% water). Retention times of synthetic standards were: INHOHBA, 18.7 min; INH<sub>2</sub>BA, 24.7 min; INO<sub>2</sub>BA, 34.5 min; INOBA, 36.5 min; and 6,6'-diiodo-3,3'-dicarbamoylazoxybenzene, 46.9 min.

## RESULTS

### In vitro chemical reactivities of NOBA and INOBA with reduced ascorbic acid and with GSH

Both NOBA and INOBA (5.8 mM in aqueous EtOH at 25°) were reduced rapidly (decolorized within 5 sec) to the corresponding hydroxylamines by 1 equiv and 10 equiv of unbuffered ascorbic acid (Eq. 1). Monitored by TLC, no amine or condensation side-products were observed within a period of several hours. Buffered at pH 7.4 resulted in no essential change in reactivity or products.

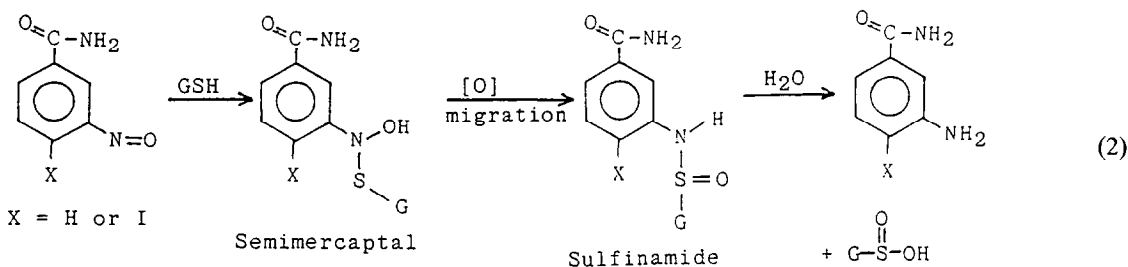


Compared with ascorbic acid, unbuffered GSH (1 equiv) reacted slower (1–2 min) with the two nitroso compounds, and gave metastable hydrophilic adducts, detectable on TLC, which then produced the respective noniodo- and iodo-amines (Eq. 2). However, the rate of production of the iodo-amine was much faster ( $T_{1/2}$  of about 10 min) than that of the noniodo-amine ( $T_{1/2}$  of about 4 hr). Increasing the

only reduction product was the amino compound (see Eq. 2).

#### Metabolic conversion of $\text{INO}_2\text{BA}$

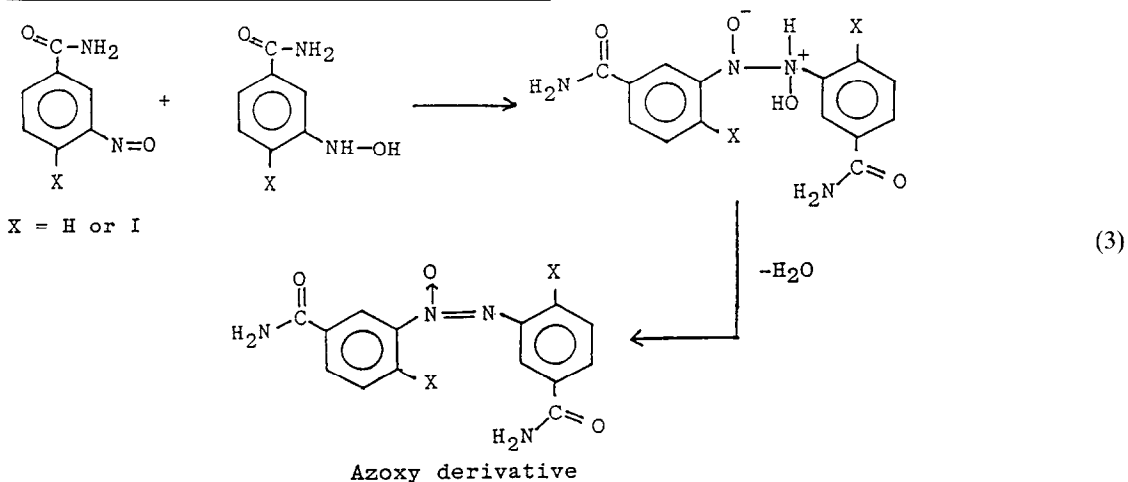
*In vitro* conversion of  $\text{INO}_2\text{BA}$  to  $\text{INH}_2\text{BA}$  by 855-2 cells (Table 1, No. 13) was determined in cell metabolism experiments (see Materials and Methods). A slow but apparently steady reduction of the nitro to the amino end-product occurred at a



Overall reaction rate is  $\text{I} \gg \text{H}$

concentration of GSH 10-fold accelerated the formation of the initial glutathione adducts (decolorization within 5–10 sec) but did not affect the rates of amine production. It is known [11–13] that GSH adds to aromatic nitroso compounds to form labile adducts (semimercaptals) (Eq. 2), one of whose reaction pathways is molecular rearrangement (oxygen atom migration) to yield sulfinamides that hydrolyze to the corresponding amines plus glutathione sulfonic acid (Eq. 2). In aqueous EtOH medium, no condensation products were present. The prerequisite for azoxy formation by condensation appears to be the simultaneous presence of nitroso and hydroxylamine species (Eq. 3), which can occur during either synthesis or reduction of the nitroso compound.

rate of  $2.2 \pm 0.2\%$  per 18 hr of cell incubation at  $37^\circ$ . The 855-2 cell line was chosen for drug metabolism studies because this cell line was most sensitive to the prodrug, and it could also be cultured on a large scale. Although not reported here in detail, preliminary results indicated that the rate of reduction of the nitro group to nitroso appeared to run parallel with cell toxicity in all cell lines studied thus far (unpublished results). Apart from as yet unidentified trace metabolites, the only identified metabolite was  $\text{INH}_2\text{BA}$  (see Eq. 2). As would be predicted from Table 1, it is likely that the rate of accumulation of the obligate nitroso metabolite may be augmented by BSO. However,  $120 \mu\text{M}$   $\text{INO}_2\text{BA}$  plus BSO produced 95% cell killing; thus, analytical demonstration of nitroso accumulation in the



When the medium for reaction with GSH was buffered at pH 7.4, NOBA and INOBA reacted at nearly the same rates (i.e. within 10 min) giving their respective hydroxylamines, and with limited GSH (1 equiv), their azoxy derivatives (Eq. 3) were detected. However, in cellular systems, hydroxylamine and azoxy species were not observed, and the

presence of BSO was not possible. Nonetheless, the removal of GSH by BSO probably augments the rate of accumulation of INOBA from  $\text{INO}_2\text{BA}$  by decreasing the rate of removal by GSH, as deduced from the pathway shown in Eq. 2. It should be noted that in repeated (triplicate) HPLC and TLC analyses no other major product but  $\text{INH}_2\text{BA}$  was identified

Table 1. Potentiating effect of DL-buthionine sulfoximine (BSO) on cytotoxicity of INO<sub>2</sub>BA in various cancer cell lines

No.	Cell line	I <sub>50</sub> (μM)		LC <sub>100</sub> (μM)	
		INO <sub>2</sub> BA	INO <sub>2</sub> BA + BSO	INO <sub>2</sub> BA	INO <sub>2</sub> BA + BSO
1	MDA-468	80	15	180	40
2	MCF-7	100	16	200	30
3	MCF-7-B-ADR	90	16	220	45
4	Du 145	120	20	250	50
5	HT 144	100	15	200	35
6	Hep-G2	120	20	200	45
7	PC-12	60	16	120	50
8	L 1210	128	20	256	64
9	CEM-4	80	15	196	32
10	HL 60	70	8	125	16
11	Molt-4	70	15	196	32
12	U 937	65	8	150	16
13	855-2	40	3	90	9

The concentration of BSO was 0.1 mM for 855-2 cells 0.25 mM for HT 144 cells, and 1 mM for all other cell lines. Cells were seeded (in the recommended growth medium) at a density of  $1.5 \times 10^4$  cells/cm<sup>2</sup> into 2-cm<sup>2</sup> wells; drugs were added simultaneously 4 hr after seeding, and incubation was continued for 48 hr (37°, 5% CO<sub>2</sub>). For assessment of drug effects, cells were detached by trypsinization and counted in a hemacytometer. Cell line Nos. 1–4 were obtained from Dr. C. Benz (University of California, San Francisco). MDA-468 and MCF-7 are human mammary cancer lines; MCF-7-B-ADR is a drug-resistant mammary cancer line; Du 145 is a drug-resistant human prostate cancer line. HT 144, a human melanoma cell line; Hep-G2, a human hepatocellular carcinoma line; and PC-12, a rat pheochromocytoma line, were obtained from University of California, San Francisco, cell culture facility. Each value is an average of two parallels that did not deviate from the average by more than  $\pm 15\%$ .

as the main metabolic product of INO<sub>2</sub>BA, indicating that the nitroso intermediate is a transient species.

#### Inactivation of pADPRT by NOBA and INOBA and concomitant zinc ion ejection

The purpose of these model experiments was to establish that the intermediate reduction product of INO<sub>2</sub>BA (i.e. INOBA) had an effect similar to that of NOBA [1] on the homogeneous pADPRT enzyme [14, 15] *in vitro*. As shown in Fig. 1 under comparable *in vitro* conditions, INOBA was the more effective inactivator of pADPRT.

Consistent with these results, zinc ejection from one zinc finger of pADPRT, as assayed after a 2-hr preincubation with either NOBA or INOBA, was complete, in agreement with the rates of enzyme inactivation, confirming earlier results [1] which show that oxidative inactivation of one zinc finger in pADPRT is sufficient to render this enzyme inactive (Fig. 2A). The zinc-ejecting activities of NOBA and INOBA were also tested in transblotted pADPRT, where zinc-ejection and loss of protein-bound Zn<sup>2+</sup> were assayed simultaneously (Fig. 2B).

Since the most striking response to zinc-ejecting C-nitroso ligands of pADPRT was DNA unwinding and fragmentation, we tested INO<sub>2</sub>BA for this effect on a variety of tumor cells. We found that exposure of AA-2 leukemia cells at  $2 \times 10^5$  cells/mL for 18 hr to 20 and 80 μM prodrug produced 12 and 40% DNA unwinding, which was comparable to the effect of NOBA as reported previously [6].

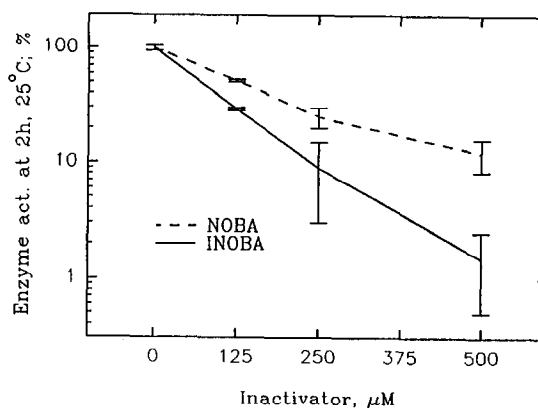


Fig. 1. Comparison of inactivation of pADPRT by NOBA and INOBA. Inactivation was performed in 20-μL volumes of buffer containing 50 mM HEPES (pH 7.4), 100 mM KCl, 0.5 mM EDTA, pADPRT (0.4 μg/μL) and different concentrations of inactivators. Inactivators were serially diluted into the above buffer from a 20 mM stock solution in DMF. The DMF concentration (2.5%) was kept constant in the inactivation mixes. After 2 hr at 25°, aliquots (3 μL) were removed for assay of enzyme activity by diluting in a volume of assay mix (200 μL) in which the inactivators were sufficiently diluted so not to act as inhibitors. The assay mix consisted of 100 mM Tris (pH 7.7), 14 mM 2-mercaptoethanol, 0.1 mM [<sup>32</sup>P]NAD<sup>+</sup>, 0.2 mg/mL coDNA and 0.1 mg/mL histones. The incorporated <sup>32</sup>P, which is proportional to enzyme activity, is plotted as a percentage of the untreated sample.

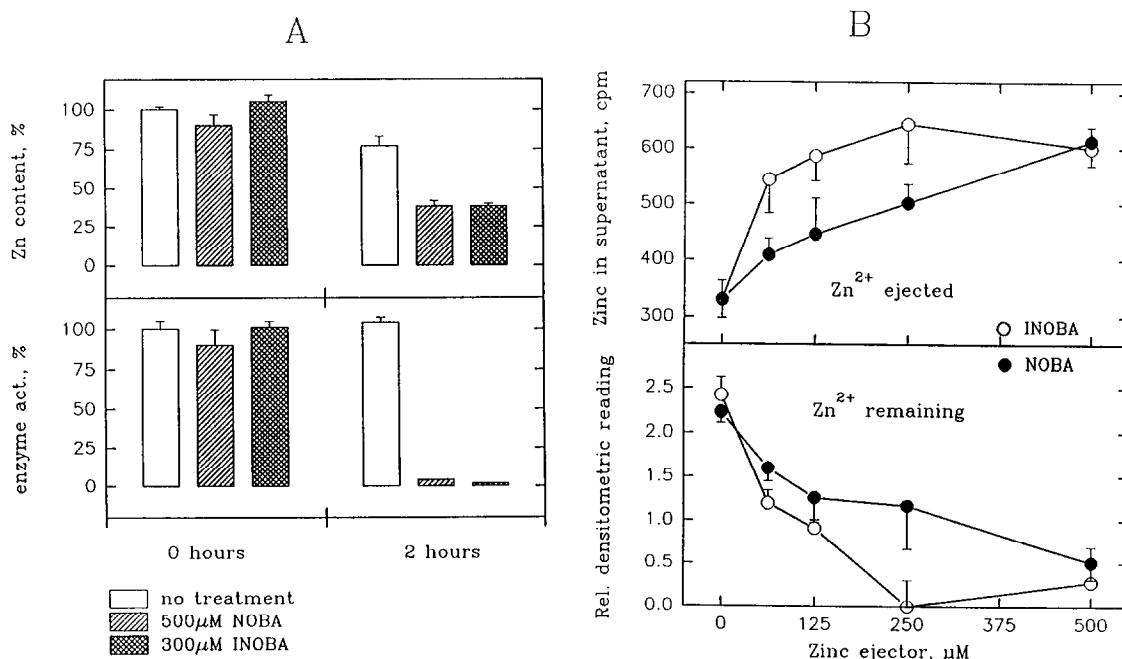


Fig. 2. Comparison of the effects of NOBA and INOBA on the enzyme activity and  $\text{Zn}^{2+}$  content of pADPRT. (A) Inactivation was performed as described in Fig. 1. In these experiments,  $^{65}\text{Zn}^{2+}$ -loaded pADPRT was used. The  $\text{Zn}^{2+}$  content of pADPRT (upper panel) was determined as follows: two parallels of aliquots ( $4\ \mu\text{L}$ ) were pipetted into  $500\ \mu\text{L}$  of ice-cold washing solution [ $50\ \text{mM}$  Tris (pH 7.7),  $10\ \text{mM}$  2-mercaptoethanol and  $0.5\ \text{mM}$  EDTA], then filtered onto GF/C disks presoaked in washing solution (cold), quickly washed four times with  $1\ \text{mL}$  of ice-cold washing solution, and dried; then radioactivity was determined. The protein-bound  $^{65}\text{Zn}^{2+}$  is shown as a percentage of the untreated sample. Enzyme assays (lower panel) were performed as described in the legend of Fig. 1. (B) For the release of  $\text{Zn}^{2+}$  from transblotted pADPRT, the enzyme ( $3\ \mu\text{g}/\text{lane}$ ) was separated on SDS-PAGE, transblotted onto a nitrocellulose membrane, and renatured in the presence of  $^{65}\text{ZnCl}_2$  ( $5\ \mu\text{Ci}$ ). The  $\text{Zn}^{2+}$ -loaded transblot was cut into strips and incubated with  $2\ \text{mL}$  of  $50\ \text{mM}$  HEPES/NaOH (pH 7.0) and  $0.5\ \text{mM}$  EDTA containing different concentrations of either NOBA or INOBA as indicated, for  $2\ \text{hr}$  at  $25^\circ$ . After incubation,  $1\ \text{mL}$  of the supernatant was counted for radioactivity, and the strips were washed three times with  $2\ \text{mL}$  of  $50\ \text{mM}$  Tris-HCl (pH 7.4),  $0.5\ \text{mM}$  EDTA and  $10\ \text{mM}$  2-mercaptoethanol, and then dried and exposed to X-ray film. The intensity of the autoradiographic spots was quantitated by a scanner.

Because of the *in vitro* reactivity of the nitroso group in INOBA with ascorbate and with GSH, we compared the cell killing effect of NOBA with the action of the prodrug  $\text{INO}_2\text{BA}$  in the presence of ascorbate, added simultaneously with both drugs. As shown in Table 2,  $160\ \mu\text{M}$  ascorbate, which by itself had no effect on AA-2 leukemia cells, completely protected against the cell death-inducing action of NOBA, but did not prevent cell killing by  $\text{INO}_2\text{BA}$  after  $18\ \text{hr}$  of drug exposure. These results are readily explained by the rapid chemical reduction of the nitroso group in NOBA to the hydroxylamine, and the rapid cellular oxidation of ascorbate to its oxidized form. Since the generation of INOBA from its prodrug is slow and steady, it would be expected that the capacity of the prodrug to induce cell death would be sustained for the entire duration of the incubation ( $18\ \text{hr}$ ). On the contrary, the rapid oxidative removal of the ascorbate takes place in minutes; thus, its protective effect is of short duration only. These results, however, predict that a chemotherapeutic efficiency of the prodrug would be much greater in species that do not synthesize ascorbate.

The role of cellular GSH was determined by the simultaneous addition of the prodrug plus an inhibitor of GSH biosynthesis, BSO [16], which was

Table 2. Effect of ascorbate on the cytotoxic action of NOBA and  $\text{INO}_2\text{BA}$

	Cell number ( $\times 10^6/\text{mL}$ )	
	Day 1	Day 2
Control	0.51	0.90
Ascorbate ( $160\ \mu\text{M}$ )	0.48	0.85
NOBA ( $32\ \mu\text{M}$ )	0.29	0.37 (50% dead)
NOBA + ascorbate	0.57	0.91
$\text{INO}_2\text{BA}$ ( $16\ \mu\text{M}$ )	0.25	0.45 (40% dead)
$\text{INO}_2\text{BA}$ + ascorbate	0.27	0.50 (40% dead)

AA-2 cells were seeded at a density of  $0.2 \times 10^6$  cells/mL. Drugs and/or sodium ascorbate were added at the time of seeding, and cells were counted by a hemacytometer after incubation ( $37^\circ$ ,  $5\% \text{CO}_2$ ) for  $18\ \text{hr}$  (Day 1) and for  $42\ \text{hr}$  (Day 2). Viability was evaluated by trypan blue exclusion. Assays were performed in triplicates, and deviation from averages did not exceed  $\pm 15\%$ .

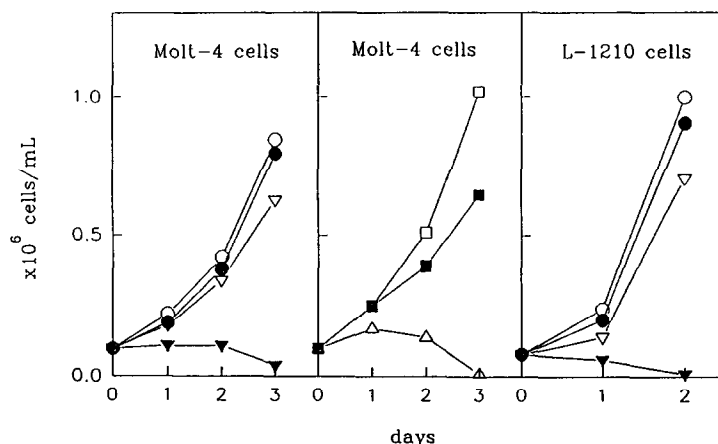


Fig. 3. Time course of cell killing by prodrugs and by NOBA. Molt-4 cells were seeded at a density of  $0.05 \times 10^6$  cells/mL in the recommended growth medium in the absence or the presence of drugs as indicated. Cells were incubated at  $37^\circ$  in a 5%  $\text{CO}_2$  atmosphere, and proliferation was monitored in 14 hr by cell counting in a hemacytometer. Key: (○) untreated control; (●) treated with  $4 \mu\text{M}$  4-iodo-3-nitrobenzoic acid; (▽) treated with 1 mM BSO; (▼) treated with  $4 \mu\text{M}$  4-iodo-3-nitrobenzoic acid and 1 mM BSO; (□) treated with  $4 \mu\text{M}$   $\text{INO}_2\text{BA}$ ; (■) treated with 1 mM BSO; and (△) treated with  $4 \mu\text{M}$   $\text{INO}_2\text{BA}$  and 1 mM BSO. L-1210 cells were seeded at a density of  $0.05 \times 10^6$  cells/mL either from untreated stock suspensions or from 24-hr pretreated ( $0.2 \times 10^6$  cells/mL) suspensions. Key: (○) untreated control; (●) treated with  $5 \mu\text{M}$  NOBA; (▽) treated with 1 mM BSO; and (▼) 24-hr pretreatment with 1 mM BSO, then treated with  $4 \mu\text{M}$   $\text{INO}_2\text{BA}$ . Each value is the mean of three parallel experiments, and the deviation from the mean was not more than 15%.

found, at the concentrations applied, to diminish cellular GSH levels below 5–10% of controls (data not shown). As summarized in Table 1, eight types

Table 3. Effect of  $\text{INO}_2\text{BA}$  on cell growth as a function of cell density

A. $I_{50}$ of $\text{INO}_2\text{BA}$ for cells growing in log phase		
	$I_{50}$ ( $\mu\text{M}$ )	
	No BSO	+ 1 mM BSO
CHO ( $8 \times 10^3$ cells/cm $^2$ )	80	10
Molt-4 ( $8 \times 10^4$ cells/mL)	25	1.5
B. Differential sensitivity of tumor cells to $\text{INO}_2\text{BA}$ at high cell density		
	$I_{50}$ ( $\mu\text{M}$ )	
	No BSO	+ 1 mM BSO
CHO (confluent, $3 \times 10^5$ cells/cm $^2$ )	150	50
Molt-4 (high density, $1.5 \times 10^6$ cells/mL)	80	10

Cells were seeded at the indicated densities, drugs were added at the time of seeding, and the effects were evaluated after 48 hr of incubation under standard conditions by counting of viable cells by hemacytometry. The deviation from the mean in three parallel experiments did not exceed  $\pm 15\%$ .

of human cancer cells, cultured as monolayers, and five types of leukemia cells, grown as suspension cultures, responded to BSO by a dramatic increase in the cell death-inducing potency of  $\text{INO}_2\text{BA}$ . Notable were the drug-resistant MCF-7-B-ADR (Adriamycin®-resistant) human mammary cancer cell line and the Du 145 drug-resistant prostatic cancer cell line.

The time-course of the onset of cell death in Molt-4 and L-1210 cells is illustrated in Fig. 3. In all cases, a combination of BSO and the  $\text{INO}_2\text{BA}$  produced rapid apoptosis as followed for 2–3 days; neither the prodrug nor BSO alone had any significant effect. In Molt-4 cells, the apoptosis-inducing action of  $\text{INO}_2\text{BA}$  and its acid analog, 4-iodo-3-nitrobenzoic acid, were indistinguishable (compare Molt-4 panels of Fig. 3), indicating that the pADPRT-inactivating action of the amide appeared to play no role in the process of cell death induction. It is noteworthy that the degree of auto-poly-ADP-ribosylation of pADPRT varies, depending on the cancer cell line [17], and in certain cells nearly all pADPRT is already unmodified before addition of the inhibitor. In that case (e.g. Molt-4), inactivation of the enzymatic function of pADPRT would have little or no consequence, and cell death is most likely to be correlated to the action of metabolically generated nitroso species at a site different from pADPRT (see Discussion). However, the majority of cancer cells respond to the amide prodrug 100–400% more, i.e. the amide prodrug is a far more effective inducer than its acid analog, indicating that both pADPRT and another nitroso-sensitive site are both participatory in the mechanism of apoptosis induction [6].

In experiments with cell cultures thus far, we determined the cell death-inducing potency in logarithmically growing cells. It was of interest to compare drug effects in cells that exhibit exponential growth with those at high cell density. With cells showing contact inhibition (e.g. CHO cells) and high density overgrowing malignant phenotype (Molt-4 tumor cells),  $I_{50}$  values of INOBA varied according to cellular growth behavior. A differential drug sensitivity of Molt-4 cells versus CHO cells was also apparent, and BSO in all instances increased the drug effects (Table 3).

The *in vivo* tolerance of twelve Syrian hamsters toward the prodrug was remarkably high, as 200 mg/kg INO<sub>2</sub>BA i.p. daily for 7 days produced no apparent ill effects in any of the animals.

### DISCUSSION

The results obtained with cell cultures are consistent with the prodrug function of INO<sub>2</sub>BA, generating the tumoricidal molecule INOBA. Published interpretations of cellular effects and pharmacology of nitro and nitroso compounds are complicated by the plethora of varied experimental procedures carried out in different biochemical systems [18]; thus, application to particular molecules requires individual analysis [19]. The toxicity and mutagenicity of 1-methyl-2-nitrosoimidazole [20] represent the behavior of a different class of compounds, and their mechanism of action is most probably related to their instability at neutral pH [21], a property not shared by the benzene C-nitroso compounds dealt with in our experiments. On the benzene ring, iodo-substitution in the position *ortho* to a nitro group has been shown to facilitate the electrochemical reduction of the nitro group [22]. Thus, it is highly probable that the metabolic reduction of INO<sub>2</sub>BA in tumor cells, although slow, is activated by the presence of the iodo group *ortho* to the nitro group. We have tested the fluoro-, chloro-, and bromo-analogs of INO<sub>2</sub>BA and found these less effective than the iodo compound, and the unsubstituted nitrobenzamides are at least 10–15 times less effective than INO<sub>2</sub>BA (unpublished results). The subcellular mechanisms of nitro group reduction [23] have been studied in cell extracts and cell particles, where an NADPH-flavoprotein-metalloprotein electron transfer system reduces the nitro group, and O<sub>2</sub> inhibits this metabolic pathway. Comparison of subcellular extracts with the operation of cellular systems provides only approximations, and erroneous interpretations of cellular metabolism are quite possible. For example, we have shown that isolated cytochrome P450 *in vitro* can oxidize the amino group of 6-amino-1,2-benzopyrone to the nitroso product [1], yet intact cells do not perform this reaction (unpublished results) indicating that the cellular actions of 6-amino-1,2-benzopyrone [17] are not due to the nitroso metabolite. Similar

uncertainty exists if the enzymatic reduction of INO<sub>2</sub>BA is to be explained on the basis of experiments performed in subcellular systems [23]. The very slow rate of reduction of the INO<sub>2</sub>BA prodrug by intact tumor cells is more in line with a competition of O<sub>2</sub> utilization with nitro group reduction [23]. It is known that the main path of aerobic NADPH oxidation is impaired in undifferentiated cells [24], and thus tumor cells may have a relatively increased ability to reduce the nitro group in INO<sub>2</sub>BA because the competing O<sub>2</sub> path is missing. If this situation exists *in vivo*, a question presently under investigation, the selective toxicity of INO<sub>2</sub>BA toward tumor cells may provide an additional chemotherapeutic advantage. The increased oxidative ability of INOBA as compared with NOBA, illustrated by the increased inactivation of pADPRT (Fig. 1) and zinc ejection (Fig. 2), is most probably explained by the *ortho* effect [25] of the iodo group, which increases the reduction potential of the nitroso group and, thus, its oxidative power. The steric consequence of the *ortho*-iodo group, forcing the nitroso group out of co-planarity with the benzene ring [25], would be greater than that of other, smaller halogens, and greatest when compared with the *ortho*-hydrogen in unsubstituted NOBA. An enhanced oxidative power of the INOBA metabolite of the prodrug may also be the basis for oxidation apparently following the path shown in Eq. 2, with no accumulation of hydroxylamine intermediate.

The large discrepancy between the concentration of nitroso compounds used in enzymological model experiments (Figs. 1 and 2) as compared with cellular studies may be explained as follows. In cellular systems the drugs enter by diffusion [6] and accumulate in the nuclear matrix; thus, the actual local concentration of drugs in the matrix, where pADPRT resides, may be high. The relatively slow onset of apoptosis (6–18 hr) is probably due to the slow rate of reduction of the prodrug and subsequent accumulation of the nitroso species in the nuclear membranes, a mechanism to be further analyzed experimentally *in vivo* [6]. If this effect is mimicked with isolated pADPRT within 2 hr, application of higher drug concentration seems reasonable.

The mechanism of induction of tumor cell killing by INOBA proceeds by the activation of endonuclease-catalyzed degradation of genomic DNA (cf. Ref. 6). However, several details of this process became clarified only recently. We find that INOBA exerts its cellular action on two levels\*. One is at the level of pADPRT by inactivation of the enzyme by zinc ejection. The second, at a site that has not yet been biochemically characterized, comprises an induction of an pADPRT-degrading aminopeptidase that completely digests pADPRT, whereby the pADPRT-binding sites on DNA become available to endonucleolytic degradation.\* Auto-poly-ADP-ribosylation protects pADPRT from digestion by aminopeptidase; hence, inactivation of poly-ADP-ribosylation (as by INOBA) is a prerequisite of proteolytic pADPRT degradation, leading to cell death.

Inasmuch as we find that some malignant cell types contain pADPRT, which is *not* auto-poly-

\* Buki KG, Bauer PI, Varadi G, Kirsten E and Kun E. Proteolytic enzymes acting on poly(ADP-ribose) polymerase: Constitutive endopeptidase and inducible aminopeptidase. Submitted for publication.



ADP-ribosylated in the intact cell [17], a structural analog of INOBA not containing the carboxamide group, 4-iodo-3-nitrosobenzoic acid (via its nitro precursor), would not be expected to bind to pADPRT because only the carboxamide group effectively binds at the nicotinamide site [26]. Yet the benzoic acid analog also induced cell death (Fig. 3). In this case, cell killing would proceed solely by way of induction of the pADPRT-degrading aminopeptidase.\* However, the majority of tumor cells respond to the benzamide-containing prodrug much more readily than to the carboxylic acid. That reduction of the prodrug to its nitroso species is essential for induction of cell killing is evident from the large activating effect of BSO, which by diminishing cellular GSH decreases the rate at which GSH chemically reduces (and thus inactivates) the nitroso molecules generated.

There is significant dependence of the concentration/cell killing ratio on the rate of cell growth and cell density (Table 3). These results imply that drug concentration alone appears insufficient to define chemotherapeutic activity, and the drug concentration/cell mass ratio becomes significant; thus,  $I_{50}$  values have to take into account the cell mass (Table 3). The marked differences in  $I_{50}$  between Molt-4 (leukemia) and CHO cells and between confluent and log-phase cell density indicate a tendency towards selective toxic action in exponentially growing cancer cells.

**Acknowledgements**—This research was supported, in part, by Octamer, Inc., and by the U.S. Air Force Office of Scientific Research (F49620-92-J-0232-DEF), with additional support by the SPORE in Breast Cancer Developmental Research Program (CA 58207-01). We wish to thank Dr. C. Benz and Ms. H. Asghari (University of California, San Francisco) for the *in vivo* treatment of Syrian hamsters with INO<sub>2</sub>BA.

## REFERENCES

1. Buki KG, Bauer PI, Mendeleyev J, Hakam A and Kun E. Destabilization of  $Zn^{2+}$  coordination in ADP-ribose transferase (polymerizing) by 6-nitroso-1,2-benzopyrone coincidental with inactivation of the polymerase but not the DNA binding function. *FEBS Lett* **290**: 181–185, 1991.
2. Buki KG, Bauer PI, Mendeleyev J, Hakam A and Kun E. Inactivation of the polymerase but not the DNA binding function of ADPRT by destabilization of one of its  $Zn^{2+}$  coordination centers by 6-nitroso-1,2-benzopyrone. In: *ADP-Ribosylation Reactions* (Eds. Poirier GG and Moreau P), pp. 329–333. Springer, New York, 1992.
3. Rice WR, Schaeffer CA, Harten B, Villinger F, South TL, Summers MF, Henderson LE, Bess JW Jr, Arthur LO, McDougal JS, Orloff SL, Mendeleyev J and Kun E. Inhibition of HIV-1 infectivity by zinc-ejecting aromatic C-nitroso compounds. *Nature* **361**: 473–475, 1993.
4. Chuan AJ, Killam KF Jr, Chuang RY, Rice WG, Schaeffer CA, Mendeleyev J and Kun E. Inhibition of the replication of native and 3'-azido-2',3'-dideoxythymidine (AZT)-resistant simian immunodeficiency virus (SIV) by 3-nitrosobenzamide. *FEBS Lett* **326**: 140–144, 1993.
5. Rice WG, Schaeffer CA, Graham L, Bu M, McDougal JS, Orloff SL, Villinger F, Young M, Oroszlan S, Fesen MR, Pommier Y, Mendeleyev J and Kun E. The site of antiviral action of 3-nitrosobenzamide on the infectivity process of human immunodeficiency virus in human lymphocytes. *Proc Natl Acad Sci USA* **90**: 9721–9724, 1993.
6. Rice WG, Hillyer CD, Harten B, Schaeffer CA, Dorminy M, Lackey DA III, Kirsten E, Mendeleyev J, Buki KG, Hakam A and Kun E. Induction of endonuclease-mediated apoptosis in tumor cells by C-nitroso substituted ligands of poly(ADP-ribose) polymerase. *Proc Natl Acad Sci USA* **89**: 7703–7707, 1992.
7. Kun E and Mendeleyev J. Sulfinic acid adducts of organo-nitroso compounds useful as retroviral inactivating agents, antiretroviral agents and antitumor agents. *US Patent No. 5,262,564*, 1993.
8. Chuang AJ, Killam KF, Chuang RY, Mendeleyev J and Kun E. Comparison of the cytotoxicity and antiviral effects of 3-nitrosobenzamide and 4-iodo-3-nitrosobenzamide. *Proc West Pharmacol Soc* **37**: 117–119, 1994.
9. Buki KG, Bauer PI, Hakam A and Kun E. Identification of domains of poly(ADP-ribose) polymerase for protein binding and self-association. *J Biol Chem* **270**: 3370–3377, 1995.
10. Birnboim HC and Jevcak JJ. Fluorometric method for rapid detection of DNA strand breaks in human white blood cells produced by low doses of radiation. *Cancer Res* **41**: 1889–1892, 1981.
11. Eyer P. Reactions of nitrosobenzene with reduced glutathione. *Chem Biol Interact* **24**: 227–239, 1979.
12. Umemoto A, Grivas S, Yamaizumi Z, Sato S and Sugimura T. Non-enzymatic glutathione conjugation of 2-nitroso-6-methyldipyrido[1,2-a:3',2'-d]imidazole (NO-Glu-P-1) *in vitro*: N-hydroxy-sulfonamide, a new binding form of aryl nitroso compounds and thiols. *Chem Biol Interact* **68**: 57–69, 1988.
13. Ellis MK, Hill S and Foster PMD. Reactions of nitrosobenzene with biological thiols: Identification and reactivity of glutathione-S-yl conjugates. *Chem Biol Interact* **82**: 151–163, 1992.
14. Buki KG, Kirsten E and Kun E. Isolation of adenosine diphosphoribosyltransferase by precipitation with Reactive Red 120 combined with affinity chromatography. *Anal Biochem* **167**: 160–166, 1987.
15. Bauer PI, Buki KG and Kun E. Evidence for the participation of histidine residues located in the 56 kDa C-terminal polypeptide domain of ADP-ribosyl transferase in its catalytic activity. *FEBS Lett* **273**: 6–10, 1990.
16. Meister A. Glutathione deficiency produced by inhibition of its synthesis, and its reversal; applications in research and therapy. *Pharmacol Ther* **51**: 155–194, 1991.
17. Cole GA, Bauer G, Kirsten E, Mendeleyev J, Bauer PI, Buki KG, Hakam A and Kun E. Inhibition of HIV-1 IIIb replication in AA-2 and MT-2 cells in culture by two ligands of poly(ADP-ribose) polymerase: 6-amino-1,2-benzopyrone and 5-iodo-6-amino-1,2-benzopyrone. *Biochem Biophys Res Commun* **180**: 504–514, 1991.
18. Venulet J and Van Etten RL. Biochemistry and pharmacology of the nitro and nitroso groups. In: *The Chemistry of the Nitro and Nitroso Groups. Part 2* (Ed. Feuer H), pp. 201–287. Interscience, New York, 1970.
19. Rosenkranz HS and Mermelstein R. Mutagenicity and genotoxicity of nitroarenes. All nitro-containing chemicals were not created equal. *Mutat Res* **114**: 217–267, 1983.
20. Noss MB, Panicucci R, McClelland RA and Rauth AM. Preparation, toxicity and mutagenicity of 1-methyl-2-nitrosoimidazole. *Biochem Pharmacol* **37**: 2585–2593, 1988.

21. McClelland RA, Panicucci R and Rauth AM, Products of the reductions of 2-nitroimidazoles. *J Am Chem Soc* **109**: 4308–4314, 1987.
22. Fry A, Electrochemistry of nitro compounds. In: *The Chemistry of Amino, Nitroso and Nitro Compounds and their Derivatives. Part 1*. (Ed. Patai S), pp. 319–335. John Wiley, New York, 1982.
23. Mason RP and Holtzman JL, The mechanism of microsomal and mitochondrial nitroreductase. Electron spin resonance evidence for nitroaromatic free radical intermediates. *Biochemistry* **14**: 1626–1632, 1975.
24. Trudel S, Pâquet MR and Grinstein S, Mechanism of vanadate-induced activation of tyrosine phosphorylation and of the respiratory burst in HL60 cells. Role of reduced oxygen metabolites. *Biochem J* **278**: 611–619, 1964.
25. Holmes RR, Reduction potential and effect of ortho substituents on dimerization of aromatic nitroso compounds. *J Org Chem* **29**: 3076–3078, 1964.
26. Althaus FR and Richter C, *ADP-Ribosylation of Proteins. Enzymology and Biological Significance*, Chap 2. Springer, Berlin, 1987.